Article

Self-Assembly of Patterned Monolayers with Nanometer Features: Molecular Selection Based on Dipole Interactions and Chain Length

Yanhu Wei, Wenjun Tong, and Matthew B. Zimmt

J. Am. Chem. Soc., **2008**, 130 (11), 3399-3405 • DOI: 10.1021/ja075170r

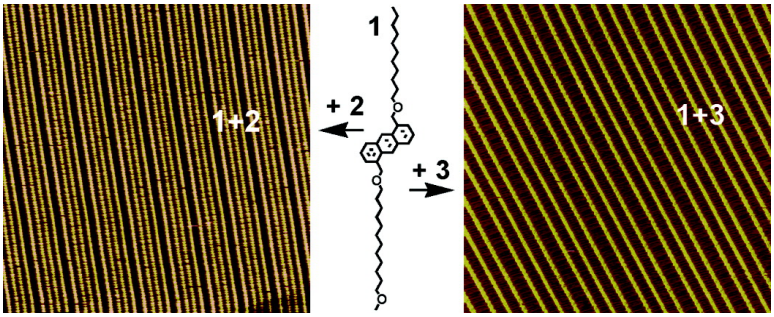

J|A|C|S
ARTICLES
Published on Web 02/27/2008

Self-Assembly of Patterned Monolayers with Nanometer Features: Molecular Selection Based on Dipole Interactions and Chain Length

Yanhu Wei,† Wenjun Tong, and Matthew B. Zimmt*

Department of Chemistry, Brown University, Providence, Rhode Island 02912

Received July 11, 2007; E-mail: mbz@brown.edu

Abstract: Patterned cocrystal monolayers self-assemble on HOPG in contact with solutions containing complementary pairs of 1,5-chain-substituted anthracene derivatives. Monolayer unit cells containing three or four molecules and spanning 9−11 nm are generated. The monolayers consist of alternating aromatic and aliphatic columns. The designs and dimensions of the cocrystal patterns (unit cells) are determined by (i) the preferred packing alignment of identical length side chains, (ii) the selectivity of each side chain for neighboring chains, (iii) the identities of the two side chains on each anthracene, and (iv) the 2D-chirality of 1,5-substituted anthracenes. The aliphatic columns form by interdigitation of identical length side chains arrayed in an antiparallel alignment, with the *n*th heavy atom of one side chain in registration with the (ω+2-n)th heavy atom of two adjacent chains (($\omega \leftrightarrow 2$) packing). Adjacent side chains are attached, alternately, to anthracenes in one of the two flanking aromatic columns. The preference for ($\omega \leftrightarrow 2$) packing optimizes side-chain van der Waals interactions. The composition and fidelity of patterning in the cocrystal monolayers requires an additional source of "molecular recognition" in addition to side-chain length. Dipolar interactions, both attractive and repulsive, between ether groups in neighboring, ($\omega \leftrightarrow 2$) packed side chains, constitute a second recognition element needed for cocrystal self-assembly.

Introduction

Surface assemblies with small feature sizes are employed in microelectronics, sensing, optical and nanotechnology applications.[1] The steadfast advance of lithographic, "top-down" technology, referred to as Moore's Law,[2] now produces complex structures with feature sizes smaller than 50 nm.[3] An alternate approach to small feature, surface construction starts at the molecular level. Self-assembly and guided assembly[4] of small molecules, polymers, biological entities, and nanoparticles constitute "bottom-up" construction methods. Two challenges facing this approach are reproducible generation of high resolution and complexly patterned surface layers to serve as templates for bottom-up assembly and expansion of template size to macroscopically useful dimensions.[5] A variety of bottom-up methods produce patterned surfaces[6] with feature resolutions in the 10 to 1000 nm range.[7] DNA-based self-assembly affords some of the highest resolution templates for "bottom-up" assembly.[8] "Double crossover" DNA components self-assemble two-dimensional (2D) scaffold monolayers, with 10−40 nm wide columns separating base-pair encoded binding sites for DNA tagged nanoparticles.[9] Designed sets of Watson−Crick base-pairing provide the critical molecular recognition needed to direct monolayer assembly and particle capture.

Self-assembly of organic and organometallic compounds produce intricate morphology monolayers, with structural features and periodicities as small as 1 nm. Numerous studies have explored the dependence of monolayer morphology on structural features of the molecular building block, including its functional groups, molecular shape, and chirality.[10] The extensive studies of single-component systems facilitate efforts

† Current address: Department of Chemical and Biological Engineering, Northwestern University, Evanston, IL 60208-3113.

(1) (a) McAlpine, M. C.; Ahmad, H.; Wang, D.; Heath, J. R. *Nat. Mater.* **2007**, *6*, 379. (b) Beckman, R.; Beverly, K.; Boukai, A.; Bunimovich, Y.; Choi, J. W.; DeIonno, E.; Green, J.; Johnston-Halperin, E.; Luo, Y.; Sheriff, B.; Stoddart, J. F.; Heath, J. R. *Faraday Discuss.* **2006**, *131*, 9. (c) Javey, A.; Nam, S. W.; Friedman, R. S.; Yan, H.; Lieber, Charles, M. *Nano Lett.* **2007**, *7*, 773.
(2) Moore, G. E. *Electronics* **1965**, *38*, 114−117.
(3) (a) http://www.intel.com/pressroom/archive/releases/20060125comp.htm. (accessed Jan 2006). (b) http://www.intel.com/pressroom/archive/releases/20070417corp_a.htm (accessed April 2007).
(4) (a) Salaita, K.; Wang, Y.; Fragala, J.; Vega, R. A.; Liu, C.; Mirkin, C. A. *Angew. Chem.* **2006**, *118*, 7378. (b) Zhang, H.; Amro, N. A.; Disawal, S.; Elghanian, R.; Shile, R.; Fragala, J. *Small* **2007**, *3*, 81. (c) Santinacci, L.; Zhang, Y.; Schmuki, P. *Surf. Sci.* **2005**, *597*, 11.
(5) Salaita, K.; Lee, S. W.; Wang, X.; Huang, L.; Dellinger, T. M.; Liu, C.; Mirkin, C. A. *Small* **2005**, *1*, 940.
(6) Samori, P.; Yin, X.; Tchebotareva, N.; Wang, Z.; Pakula, T.; Jackel, F.; Watson, M. D.; Venturini, A.; Müllen, K.; Rabe, J. P. *J. Am. Chem. Soc.* **2004**, *126*, 3567.
(7) (a) Jung, Y. S.; Ross, C. A. *Nano Lett.* **2007**, *7*, 2046−2050. (b) Kim, H.-Ch.; Cheng, J.; Rettner, C.; Park, O.-H.; Miller, R.; Hart, M.; Sundstroem, L.; Zhang, Y. *Proceedings of SPIE-Advances in Resist Materials and Processing Technology XXIV*; Lin, Q., Ed.; SPIE: Bellingham, WA, 2007; Vol. 6519, 65191H/1. (c) Chowdhury, D.; Maoz, R.; Sagiv, J. *Nano Lett.* **2007**, *7*, 1770−1778. (d) Tahara, K.; Furukawa, S.; Uji-i, H.; Uchino, T.; Ichikawa, T.; Zhang, J.; Mamdouh, W.; Sonoda, M.; De Schryver, F. C.; De Feyter, S.; Tobe, Y. *J. Am. Chem. Soc.* **2006**, *128*, 16613. (e) Mourran, A.; Ziener, U.; Moeller, M.; Suarez, M.; Lehn, J.-M. *Langmuir* **2006**, *22*, 7579. (f) Kikkawa, Y.; Koyama, E.; Tsuzuki, S.; Fujiwara, K.; Miyake, K.; Tokuhisa, H.; Kanesato, M. *Langmuir* **2006**, *22*, 6910−6914.
(8) (a) Winfree, E.; Liu, F.; Wenzler, L. A.; Seeman, N. C. *Nature* **1998**, *394*, 539. (b) Reishus, D.; Shaw, B.; Brun, Y.; Chelyapov, N.; Adleman, L. *J. Am. Chem. Soc.* **2005**, *127*, 17590.
(9) Pinto, Y. Y.; Le, J. D.; Seeman, N. C.; Musier-Forsyth, K.; Taton, T. A.; Kiehl, R. A. *Nano Lett.* **2005**, *5*, 2399.

to understand structure−morphology correlations in multicomponent monolayers. As discussed by Yang,[11a] Feyter,[11b] Plass,[11c] Wei,[11d] and Tao,[11e] mixtures of molecules can assemble monolayers of three (limiting) types: phase segregated, randomly mixed, or cocrystallized. The monolayer components' shapes, interaction strengths, concentrations, and solubilities are important factors determining the fraction of each monolayer type present at equilibrium.[11] Randomly mixed (doped) assemblies have been used to characterize single molecule properties and the dynamics of monolayers.[12] At the other extreme, cocrystallization is potentially useful for assembling complex monolayers, in which composition varies among neighboring molecules (1−3 nm features) while producing periodicity that extends over many molecules (>10 nm). Rabe and Müllen were the first to demonstrate rational, two-component, monolayer patterning (cocrystallization) by exploiting the strong hydrogen bond between 5-alkoxyisophthalic acids and -pyrazine derivatives.[13] Numerous subsequent studies have explored two-component coadsorption driven by hydrogen bonding.[14] "Host−guest" assemblies are a second class of patterned, cocrystal monolayers, in which large, aromatic guests (e.g., coronene, triphenylene, phthalocyanine) adsorb at surface vacancies present,[15a,b] or induced,[15c] in template monolayers. Adsorption of the large guest molecules at preexisting vacancies in the template is driven, presumably, by favorable guest−surface and guest−host interactions and by increased entropy accompanying release of multiple solvent molecules from the surface vacancies. Plass et al.[11c] reported a third class of cocrystal monolayers.[16] These cocrystals assemble from a mixture of phthalate and isophthalate esters whose single-component monolayers exhibit very different morphologies.[11c] The cocrystal unit cells are large, consisting of as many as eight molecules and extending as long as 12 nm. As is true for host−guest cocrystals in which guest binding alters the host morphology, the morphology of the phthalate/isophthalate cocrystals is difficult to predict based on the pure component monolayers' morphologies.

We recently reported a designed approach to 2D-cocrystallization that utilizes dipole−dipole interactions to self-assemble monolayers with alternating composition of neighboring columns of molecules.[17] This patterning approach exploits the preferred monolayer packing of 1,5-bis-(side chain)-anthracenes, in which the terminal methyl group (ω-position) of each linear side chain lies in registration and in van der Waals contact with the group (CH_2, O, S) at the 2-position of two neighboring side chains [referred to as "($\omega \leftrightarrow 2$)-packing", Chart 1, bottom]. The assembled monolayers consist of single-lamella domains[18] containing columns of anthracene cores separated by columns of interdigitated side chains.[7d,19] Directed cocrystallization was achieved by positioning two dipolar ether groups in each side chain such that ($\omega \leftrightarrow 2$)-packing of identical side chains generated two sets of repulsive dipolar interactions (self-repulsive side chains). By contrast, ($\omega \leftrightarrow 2$)-packed side chains with complementary positioning of ether groups enjoyed two sets of attractive dipolar interactions. Each anthracene in the prior demonstration was symmetrically 1,5-disubstituted with one self-repulsive side chain. Cocrystallization required each side chain to select and coadsorb its dipolar complement as its two neighboring chains. In this contribution, designed monolayer cocrystals assemble at the liquid−HOPG interface from a solution containing two unsymmetrical anthracenes. Cocrystal formation requires each side chain to select its neighbors from, as many as, four distinct side chains present in solution. Chain length matching combines with dipolar selection to provide the recognition and selection required for cocrystallization. Varying the anthracene components' symmetries and chain lengths alters the self-assembled monolayer morphology and cocrystal unit cell properties in a predictable manner.

Experimental Section

Scanning tunneling microscopy data was acquired using a Digital Instruments NanoScope STM interfaced to a Digital Instruments NanoScope IIIa controller. All data was collected from the solution−graphite interface (HOPG, ZYB grade, Momentive Performance, Strongsville, OH) using mechanically cut 87/13 Pt/Rh tips (0.25 mm, Omega Engineering, Stamford, CT). Sample solutions were prepared by dissolving 5−15 mg of compound in 250 μL of phenyloctane (Aldrich, 98%) at 22 °C. Solutions were diluted (adding 0−250 μL phenyloctane), filtered (Anatop Plus 0.02 μm filters, Whatman), and equilibrated at the temperature of the STM room (16−20 °C). A solution

(10) (a) Walba, D. M.; Stevens, F.; Clark, N. A.; Parks, D. C. *Acc. Chem. Res*. **1996**, *29*, 591−597. (b) Claypool, C. L.; Faglioni, F.; Goddard, W. A., III; Gray, H. B.; Lewis, N. S.; Marcus, R. A. *J. Phys. Chem. B* **1997**, *101*, 5978−5995. (c) Giancarlo, L. C.; Flynn, G. W. *Acc. Chem. Res*. **2000**, *33*, 491−501. (d) Yin, S.; Wang, C.; Xu, Q.; Lei, S.; Wan, L.; Bai, C. *Chem. Phys. Lett*. **2001**, *348*, 321−328. (e) Plass, K. E.; Kim, K.; Matzger, A. J. *J. Am. Chem. Soc*. **2004**, *126*, 9042−9053. (f) Tao, F.; Bernasek, S. L. *J. Phys. Chem. B* **2005**, *109*, 6233−6238. (f) Zell, P.; Mçgele, F.; Ziener, U.; Rieger, B. *Chem. Eur. J*. **2006**, *12*, 3847−3857. (g) Mu, Z.; Wang, Z.; Zhang, X.; Zhang, X.; Ye, K.; Wang, Y. *J. Phys. Chem. B* **2004**, *108*, 19955−19959.

(11) (a) Yang, X.; Mu, Z.; Wang, Z.; Zhang, X.; Wang, J.; Wang, Y. *Langmuir* **2005**, *21*, 7225−7229. (b) De Feyter, S.; Larsson, M.; Schuurmans, N.; Verkuijl, B.; Zoriniants, G.; Gesquière, A.; Abdel-Mottaleb, M. M.; van Esch, J.; Feringa, B. L.; van Stam, J.; De Schryver, F. *Chem. Eur. J*. **2003**, *9*, 1198−1206. (c) Plass, K. E.; Engle, K. M.; Cychosz, K. A.; Matzger, A. J. *Nano Lett*. **2006**, *6*, 1178−1183. (d) Wei, Y.; Tong, W.; Wise, C.; Wei, X.; Armbrust, K.; Zimmt, M. *J. Am. Chem. Soc*. **2006**, *128*, 13362−63. (e) Tao, F.; Bernasek, S. L. *Surf. Sci*. **2007**, *601*, 2284−2290.

(12) (a) Padowitz, D. F.; Sada, D. M.; Kemer, E. L.; Dougan, M. L.; Xue, W. A. *J. Phys. Chem. B* **2002**, *106*, 593−598. (b) Papadantonakis, K. M.; Brunschwig, B. S.; Lewis, N. S. *Langmuir* **2008**; ASAP Article. (c) Donhauser, Z. J.; Mantooth, B. A.; Kelly, K. F.; Bumm, L. A.; Monnell, J. D.; Stapleton, J. J.; Price, D. W., Jr.; Rawlett, A. M.; Allara, D. L.; Tour, J. M.; Weiss, P. S. *Science* **292** (5525) 2303−2307. (d) Hallbäck, A.-S.; Poelsema, B.; Zandvliet, H. J. W. *ChemPhysChem* **2007**, *8*, 661−665. (e) Wakamatsu, S.; Fujii, S.; Akiba, U.; Fujihira, M. *Nanotechnology* **2004**, *15*, S137−S141.

(13) Eichhorst-Gerner, K.; Stabel, A.; Moessner, G.; Declerq, D.; Valiyaveettil, S.; Enkelmann, V.; Müllen, K.; Rabe, J. P. *Angew. Chem., Int. Ed. Engl*. **1996**, *35*, 1492−1495.

(14) (a) De Feyter, S.; Gesquiere, A.; Abdel-Mottaleb, M. M.; Grim, P. C. M.; De Schryver, F. C.; Meiners, C.; Sieffert, M.; Valiyaveettil, S.; Mullen, K. *Acc. Chem. Res*. **2000**, *33*, 520−531. (b) Mamdouh, W.; Dong, M.; Xu, S.; Rauls, E.; Besenbacher, F. *J. Am. Chem. Soc*. **2006**, *128*, 13305−13311. (c) Wintgens, D.; Yablon, D. G.; Flynn, G. W. *J. Phys. Chem. B* **2003**, *107*, 173−179. (d) Xu, S.; Yin, S.-X.; Liang, H.-P.; Wang, C.; Wan, L.-J.; Bai, C.-L. *J. Phys. Chem. B* **2004**, *108*, 620−624. (e) Kampschulte, L.; Griessl, S.; Heckl, W. M.; Lackinger, M. *J. Phys. Chem. B* **2005**, *109*, 14074−14078.

(15) (a) Lu, J.; Lei, S.; Zeng, Q.; Kang, S.; Wang, C.; Wan, L.; Bai, C. *J. Phys. Chem. B* **2004**, *108*, 5161−5165. (b) Griessl, S.; Lackinger, M.; Jamitzky, F.; Markert, T.; Hietschold, M.; Heckl, W. M. *Langmuir* **2004**, *20*, 9403−9407. (c) Wu, D.; Deng, K.; He, M.; Zeng, Q.; Wang, C. *ChemPhysChem* **2007**, *8*, 1519−1523.

(16) For additional examples of coadsorption without hydrogen bonding or host-guest morphology, see (a) Lei, S. B.; Yin, S. X.; Wang, C.; Wan, L. J.; Bai, C. L. *Chem. Mater*. **2002**, *14*, 2837−2838. (b) Hipps, K. W.; Scudiero, L.; Barlow, D. E.; Cooke, M. P., Jr. *J. Am. Chem. Soc*. **2002**, *124*, 2126−2127.

(17) Wei, Y.; Tong, W.; Wise, C.; Wei, X.; Armbrust, K.; Zimmt, M. *J. Am. Chem. Soc*. **2006**, *128*, 13362.

(18) (a) Alkanoic acids[18b] are another example of domains composed of a single lamella. Alkanes[18c] and alkanols[10c] form domains consisting of multiple lamellae. (b) Yablon, D. G.; Wintgens, D.; Flynn, G. W. *J. Phys. Chem. B* **2002**, *106*, 5470−5475. (c). Askadskaya, L.; Rabe, J. P. *Phys. Rev. Lett*. **1992**, *69*, 1395−1398.

(19) (a) Samori, P.; Fechtenkotter, A.; Reuther, E.; Watson, M. D.; Severin, N.; Mullen, K.; Rabe, J. P. *Adv. Mater*. **2006**, *18*, 1317. (b) Stabel, A.; Heinz, R.; Rabe, J. P.; Wegner, G.; De Schryver, F. C.; Corens, D.; Dehaen, W.; Sueling, C. *J. Phys. Chem*. **1995**, *99*, 8690.

Chart 1. Structures, Numeric, and Side-Chain Abbreviations for the Anthracene Derivatives, **1**−**4**, Employed in This Study[a]

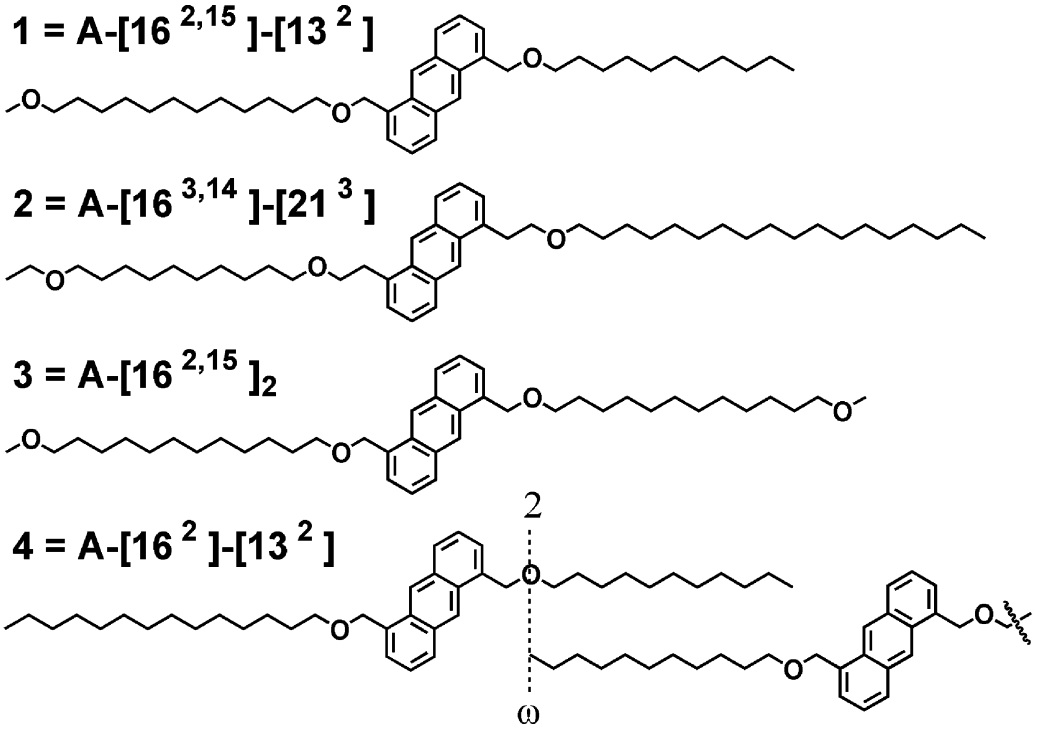

[a] The non-superscript number in a square bracket indicates the total number of carbon and oxygen atoms in a side chain. The superscripts indicate the side-chain positions of ether oxygen atoms relative to the anthracene ring. The "($\omega \leftrightarrow 2$)-packing" alignment of side-chain CH_2 and oxygen atoms is displayed for two undecyloxymethyl side chains, [13^2], of **4**.

drop was deposited on a recently cleaved HOPG surface. Samples were annealed at 40−45 °C for 1−2 h. The STM tip was engaged through the solution, and scanning was initiated in constant height mode. After monolayers appeared and tip hysteresis minimized, data collection was initiated in constant current mode with feedback parameters specified in each image. Tip scan velocities were in the range 0.20−1.2 μm/s. Data was acquired from monolayers formed from single-component or two-component mixtures (mole ratios 1:3−3:1). For internal calibration of the STM data, feedback parameters were adjusted to collect data from the graphite surface beneath the monolayer. The synthesis and characterization of compounds is reported in a thesis[20] and in the Supporting Information.

Results and Discussion

Compounds and Side-Chain Packing. Chart 1 displays the 1,5-substituted anthracene derivatives used in this study. The side-chain structures are identified by numbers in brackets: the total number of carbon and oxygen atoms is indicated by the non-superscript number. The superscripts indicate side-chain positions, relative to the anthracene ring, of ether oxygen atoms. Anthracene **1** is substituted at C-1 with a 12-methoxydodecyloxymethyl side chain, [$16^{2,15}$], and at C-5 with an undecyloxymethyl side chain, [13^2]. Anthracene **2** is substituted at C-1 with a 10-ethoxydecyloxyethyl side chain, [$16^{3,14}$], and at C-5 by an octadecyloxyethyl side chain, [21^3]. The two 16-atom side chains, [$16^{2,15}$] and [$16^{3,14}$], are each self-repulsive[17] in ($\omega \leftrightarrow 2$)-packed monolayers but comprise a complementary (attracting) pair. Anthracene **3** bears [$16^{2,15}$] chains at the 1- and 5-positions. Anthracene **4** is substituted by a tetradecyloxymethyl chain, [16^2], at C-1 and by a [13^2] chain at C-5.

Side-Chain Length-Matching: A Tool for Patterning. Unsymmetrical 1,5-substituted anthracenes are potentially useful for self-assembly of patterned monolayer cocrystals provided the two side chains select and adsorb next to different neighbor chains. STM studies reveal that interdigitated monolayers formed by alkanoic acids segregate molecules differing in length by four CH_2 groups.[21] Thus, side-chain length might function as a rudimentary molecular recognition/side-chain selection criterion for the interdigitated monolayers formed from 1,5-substituted anthracenes. Unsymmetrical anthracene **4**, with [13^2] and [16^2] side chains, affords a test of length matching's efficacy as a selection criterion for this system. Constant current STM scans (Figure 1) of the monolayer self-assembled on HOPG by **4** in phenyloctane solution reveal parallel anthracene columns separated, alternately, by [13^2] columns (2.3 nm center-to-center anthracene separation) and [16^2] columns (2.7 nm separation). Segregating side chains by length retains ($\omega \leftrightarrow 2$)-packing, maximizes side chain van der Waals attractions and, apparently, minimizes the free energy. Although monolayers defects are observed (bottom of Figure 1A), side-chain segregation based on a difference of three CH_2 units is moderately effective as a neighbor selection criterion. Despite being assembled from a single-compound, the 2D unit cell of the monolayer formed by **4** consists of four molecules (Figure 1B,C). The unsymmetrical anthracene can adsorb to HOPG via either enantiotopic face (pS, pR)[22] and with its longer side chain extended to the left (-l) or to the right (-r) of the anthracene column. The unit cell of the monolayer from **4** includes all four adsorption orientations

(20) Wei, Yanhu, Ph.D. Thesis, Brown University, 2007.

(21) Yablon, D. G.; Ertas, D.; Fang, H.; Flynn, G. W. *Isr. J. Chem.* **2003**, *43*, 383.

(22) (a) 1,5-Substituted anthracenes are prochiral (C_{2h} or C_s symmetry). Using the benzylic hydrogen pointing toward the surface as the pilot atom[22b] for the benzylic, C-1, and C-1a carbons, surface-adsorbed molecules have either pR or pS symmetry. (b) Eliel, E. L.; Wilen, S. H.; Mander, L. N. *Stereochemistry of Organic Compounds*; John Wiley & Sons: New York, 1994; Chapter 14.1.

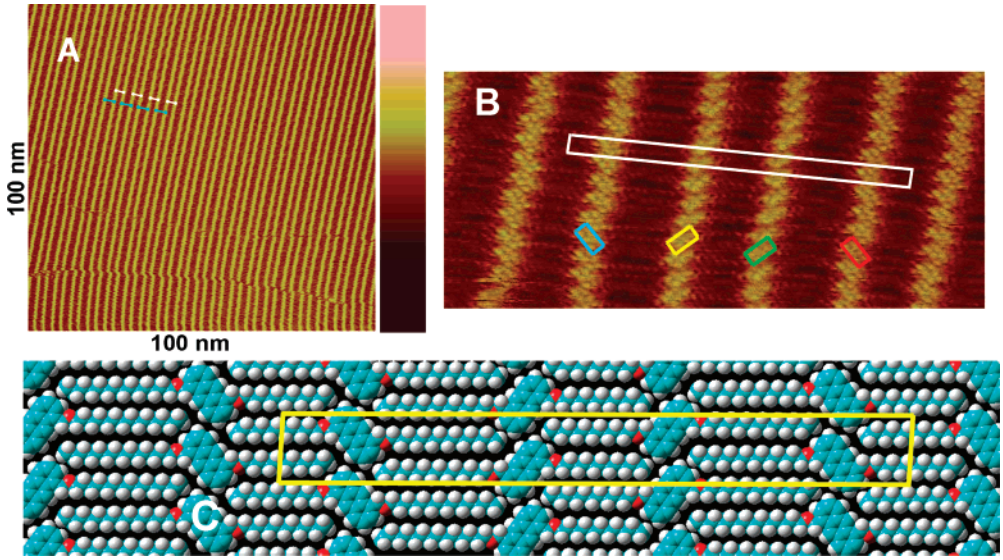

Figure 1. (A) Constant current STM scan (40 pA, 1.0 V, 100 nm × 100 nm) of the monolayer formed by a solution **4** in phenyloctane applied to HOPG. The color legend for tip-height is shown on the right: max (pink) = 0.5 nm, min (brown) = 0.0 nm. The yellow stripes are columns of anthracene groups. Blue bars mark the anthracene center-to-center separation (2.75 nm) across ($\omega \leftrightarrow 2$)-packed columns of [16^2] side chains. White bars mark the analogous distance (2.30 nm) across ($\omega \leftrightarrow 2$)-packed columns of [13^2] side chains. Two propagating line defects are evident in the bottom half of the scan. (B) Constant current, high-resolution STM scan (40 pA, 1.0 V, 16 nm × 7 nm) of **4** on HOPG. The white box highlights a unit cell of the *p*2 monolayer. The "3 × 2 dot" patterns from the anthracenes[23a,24] indicate the adsorption geometry of the molecules in each column: pS-r (blue), pR-l (yellow), pR-r (green), pS-l (red). (C) CPK cartoon of the monolayer assembled by **4**. The yellow box outlines the contents of one unit cell.

Table 1. Unit Cell Parameters of the Monolayers (measured)

compd(s)	plane group	length (nm)	width (nm)	angle (deg)	molecules per asymmetric unit
4	*p*2[a]	10.2 ± 0.4	1.0 ± 0.1	88[a] ± 4	2
1 + **2**	*p*2	11.2 ± 0.7	1.0 ± 0.1	87 ± 6	2
3 + **2**	*p*2	9.0 ± 0.5	1.0 ± 0.1	85 ± 3	1.5

[a] If the unit cell angle is exactly 90°, the plane group of the monolayer formed by **4** is *pgg*.

in the sequence (pS-r, pR-l, pR-r, pS-l) because of chain length matching and chirality effects arising from ($\omega \leftrightarrow 2$)-packing.[23] Table 1 lists the unit cell parameters.

Cocrystal Self-Assembly. Patterned cocrystal monolayers can assemble from mixtures of 1,5-substituted anthracenes provided each molecule has at least one side chain that preferentially selects neighbor chains whose structure is distinct. Given the bias *favoring* interdigitation of identical length side chains, cocrystal formation from these anthracenes requires pairs of same length side chains that *disfavor* self-assembly of single-component side chain columns and strongly *favor* self-assembly of alternating, two-component side-chain columns. As noted above, a prior study[17] using 1,5-bis-[$16^{2,15}$]-anthracene and 1,5-bis-[$16^{3,14}$]-anthracene demonstrated the requisite selectivity and the feasibility of modulating monolayer column compositions using identical length, "self-repulsive", pairwise attractive side-chain structures. The use of two C_{2h} symmetric molecules in the prior study (i) required each side chain to select its neighbors from among only two side-chain structures present in solution, (ii) produced monolayers with no obvious morphological evidence of patterning (anthracene center-to-center distances were constant), and (iii) made unambiguous assignment of the monolayer columns' compositions difficult. Here we explore the self-assembly of patterned, cocrystal monolayers using two unsymmetrical anthracenes **1** and **2,** each of which bears only one self-repulsive side chain from the [$16^{2,15}$]/[$16^{3,14}$] complementary pair. Cocrystal assembly requires each side chain to select neighbors from among four side-chain structures present in solution.

Constant current STM scans reveal a distinctly patterned monolayer cocrystal that self-assembles on HOPG from mixtures of **1** and **2** in phenyloctane (Figure 2). A low resolution, 100 nm × 100 nm image (Figure 2A) displays a repeating pattern, with centers of adjacent anthracene columns (yellow, high tunneling regions) spaced, sequentially, by 3.3−2.7−2.3−2.7 nm. This "tetrad" sequence exhibits a recurring height modulation with maximum amplitude of 4 Å (Figure 2B). The widest side-chain columns consist of ($\omega \leftrightarrow 2$)-interdigitated [21^3] chains from adjacent columns of **2** (anthracene center-to-center spacing, 3.3 nm). The narrowest side-chain columns (2.3 nm) are ($\omega \leftrightarrow 2$)-interdigitated [13^2] chains from adjacent columns of **1**. Adjacent rows of **1** and **2** are separated by 2.7 nm, consistent with the spacing produced by ($\omega \leftrightarrow 2$)-interdigitated [$16^{2,15}$] and [$16^{3,14}$] chains. Submolecular resolution scans (Figure 2C) reveal the anthracene cores as rectangular, 3 × 2 dot patterns.[23a,24] The anthracene orientations in adjoining columns confirm ($\omega \leftrightarrow 2$)-packing of the intervening side chains: odd length side-chain columns separate columns of parallel-aligned anthracenes which adsorb via the same enantiotopic face (Figure 2C: identical color rectangles); even length side-chain columns separate columns of skew-aligned anthracenes, adsorbed via opposite enantiotopic faces (Figure 2C; different color rectangles).[24a] The unit cell of this monolayer (Figure 2C,D) contains four molecules[25] and extends 11.2 nm (Table 1).

If chain length "matching" was the sole factor determining side-chain column composition in the mixed monolayer formed

(23) (a) Wei, Y.; Kannappan, K.; Flynn, G. W.; Zimmt, M. B. *J. Am. Chem. Soc.* **2004**, *126*, 5318−5322. (b) Tao, F.; Bernasek, S. L. *Chem. Rev.* **2007**, *107*, 1408−1453.

(24) Pokrifchak, M.; Turner, T.; Pilgrim, I.; Johnston, M. R.; Hipps, K. W. *J. Phys. Chem. C* **2007**, *111*, 7735−7740.

(25) The composition and orientation patterning of the selected **1**/**2** unit cell is **1**-pR-r, **2**-pS-r, **2**-pS-l, **1**-pR-l where - r or -l refer to the extension direction of the longer side chain.

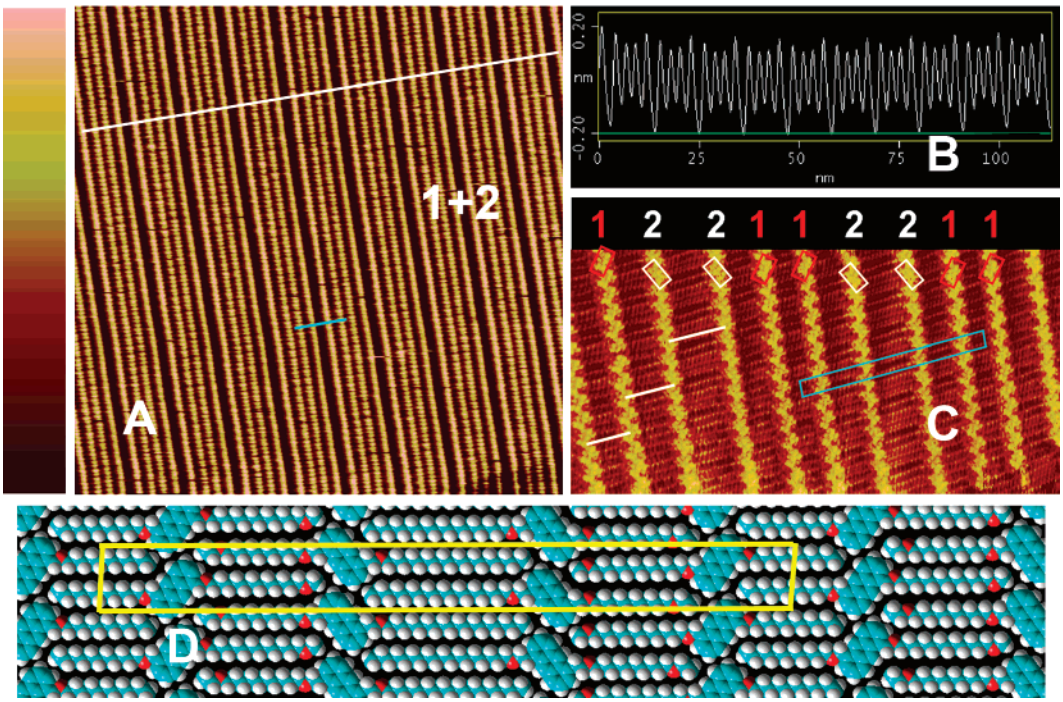

Figure 2. Constant current STM data from the patterned monolayer cocrystal formed by a mixture of **1** and **2** (1:2) in phenyloctane applied to HOPG. (A) 100 nm × 100 nm scan (0.1 nA, 1.0 V) exhibiting the tetrad repeat. (Tip-height color legend to the left: max (pink) = 0.8 nm, min (brown) = 0.0 nm.) Bright regions are the anthracene columns. The sequence of center-to-center distances between adjacent anthracene columns is 3.3 nm/2.7 nm/2.3 nm/2.7 nm. The light blue bar covers (approximately) one unit cell of the cocrystal (11.2 nm × 1.0 nm). (B) Tip height variation along the direction of the white line in part A. Height data is averaged over a 30 nm section parallel to the columns. (C) 30 nm × 15 nm constant current STM scan (50 pA, 1.0 V) exhibiting molecular details of the monolayer. The 3 × 2 dot pattern from anthracene is visible for **2** (white rectangles, pS face adsorbed) and for **1** (red rectangles, pR face adsorbed). Side-chain hydrogen atoms are visible as small yellow dots in the darker, side-chain columns. The light blue box outlines one unit cell of the cocrystal. (D) CPK cartoon of the monolayer assembled by **1** and **2**. The yellow box outlines the contents of one unit cell.

Chart 2. Dipole−Dipole Interactions in ($\omega \leftrightarrow 2$)-Packed, Diether Side-Chain Columns[a]

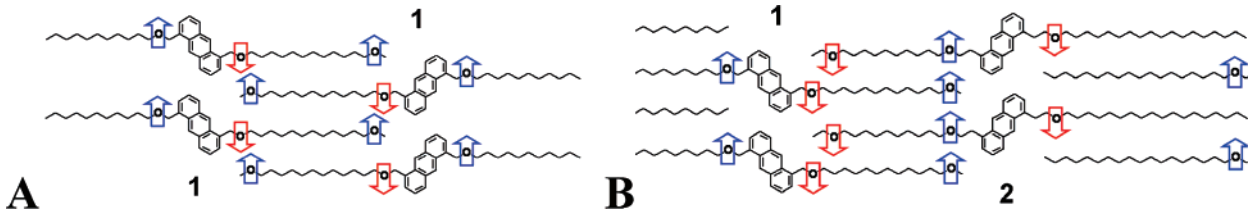

[a] Arrows indicate ether dipole directions: Blue = up, red = down. (A) For ($\omega \leftrightarrow 2$)-packed, [$16^{2,15}$] chains, both ether groups in each diether chain experience repulsive dipolar interactions with two, proximate ether dipoles from adjacent chains. (B) All proximate ether dipoles in the side chains experience attractive interactions for alternating, ($\omega \leftrightarrow 2$)-packed [$16^{2,15}$] and [$16^{3,14}$] chains.

from **1** and **2**, the 2.7 nm wide lamellae (16-atom side chains) could form from two adjacent columns of **1**, two adjacent columns of **2** or adjacent columns of **1** and **2**. Adjacent columns of **1** would exhibit 2.3 nm/2.7 nm/2.3 nm anthracene spacing sequences. Adjacent columns of **2** would exhibit 3.3 nm/2.7 nm/3.3 anthracene spacing sequences. The observed regularity of the 3.3 nm/2.7 nm/2.3 nm/2.7 nm "tetrad repeat" spacing sequence demonstrates that the [$16^{2,15}$] side chain of **1** and the [$16^{3,14}$] side chain of **2** preferentially interdigitate, forming ordered, two-component side-chain columns that drive cocrystal formation.

Probing Dipolar Interactions. Dipolar interaction between side-chain ether groups is the proposed explanation for preferential interdigitation of [$16^{2,15}$] and [$16^{3,14}$] groups within the side-chain columns.[17] As shown in Chart 2A, ($\omega \leftrightarrow 2$)-packing of adjacent [$16^{2,15}$] side chains generates repulsive, antiparallel alignment of proximate dipoles in adjacent chains. These repulsive interactions destabilize ($\omega \leftrightarrow 2$)-packed columns assembled from neighboring [$16^{2,15}$] side chains. Analogous, repulsive dipolar interactions arise for ($\omega \leftrightarrow 2$)-packed columns assembled from neighboring [$16^{3,14}$] side chains of **2**.[26] By contrast, ($\omega \leftrightarrow 2$)-packing of alternating, interdigitated [$16^{2,15}$] (**1**) and [$16^{3,14}$] (**2**) side chains generates stabilizing, parallel alignment of proximate dipoles (Chart 2B) in addition to optimal van der Waals interactions (length matching). Adjacent, identical diether chains are self-repulsive when ($\omega \leftrightarrow 2$)-packed. Dipolar stabilization from alternating, interdigitation allows the two

(26) A reviewer noted that [$16^{2,15}$] chains may interdigitate and generate dipolar stabilization by assuming ($\omega \leftrightarrow 1$)- or ($\omega \leftrightarrow 3$)-packing as previously reported for 1,5-bis-[$16^{2,15}$]-anthracene.[17] ($\omega \leftrightarrow 3$)-packing reduces van der Waals attractions between neighboring chains. ($\omega \leftrightarrow 1$)-packing generates steric repulsion between terminal methyls and anthracene cores. The destabilization of ($\omega \leftrightarrow 1$)- or ($\omega \leftrightarrow 3$)-packing relative to ($\omega \leftrightarrow 2$)-packing is the origin of the odd−even effects previously reported for anthracenes lacking dipolar groups.[23a] For pure 1,5-bis-[$16^{2,15}$]-anthracene, only one composition side chain is present; therefore, this molecule can only form single-component, side-chain columns. The experimental morphology indicates that ($\omega \leftrightarrow 2$)-packing, with the attendent dipolar repulsion, lies higher in energy than ($\omega \leftrightarrow 1$)- or ($\omega \leftrightarrow 3$)-packing. However, when [$16^{3,14}$] chains are also present in solution, ($\omega \leftrightarrow 2$)-packing of the complementary side chains is energetically preferred.

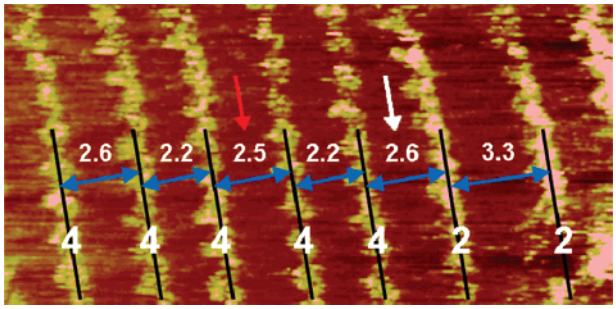

Figure 3. Constant height STM (95 pA, 0.9 V) scan of a **4**/**2** mixture (1:3) in phenyloctane applied to HOPG. The mean separations (blue arrows) between the centers of adjoining anthracene columns (bright regions superimposed by black lines) are indicated (units in nm). On the basis of the sequence of anthracene separations, the red arrow indicates a side-chain column formed from pure [16^2] (i.e., two neighboring columns of **4**). The white arrow indicates a side-chain column formed from alternating [16^2] and [$16^{3,14}$] side chains (i.e., neighboring columns of **4** and **2**).

isomeric diether chains, [$16^{2,15}$] and [$16^{3,14}$], to recognize and select each other as ($\omega \leftrightarrow 2$)-packed neighbors.

The proposed dipolar origin of patterned cocrystal formation observed in **1**/**2** monolayers (Figure 2) was investigated using **4**/**2** mixtures. The structures of **1** and **4** differ at the 15-position of the 16-atom-long side chain: **4** has a non-dipolar CH_2 group; **1** has a dipolar oxygen. As noted above, the placement of ether dipoles in the [$16^{2,15}$] side chain of **1** causes this chain to repel identical, ($\omega \leftrightarrow 2$)-packed side chains and to attract the [$16^{3,14}$] diether side chain of **2**. By contrast, the [16^2], monoether side chain of **4** attracts identical [16^2] side chains as neighbors (Figure 1) and should also attract the [$16^{3,14}$] side chain of **2**, based on length matching and one set of attractive, ether dipole interactions per pair of ($\omega \leftrightarrow 2$)-packed side chains. The [16^2] chains of **4** may form ($\omega \leftrightarrow 2$)-packed side-chain columns with adjoining molecules of **2** (side-chain column composition $\rightarrow$ alternating [16^2] and [$16^{3,14}$] chains) or with adjoining molecules of **4** (side-chain column composition $\rightarrow$ pure [16^2]). The availability of two compounds that can ($\omega \leftrightarrow 2$)-pack with the [16^2] chain of **4** should disrupt patterning fidelity and randomize the sequence of column compositions and the corresponding spacings between neighboring anthracenes.

Mixtures of **4** and **2** in phenyloctane were deposited onto HOPG. STM scans of the immediately formed monolayer revealed domain morphologies resembling pure **4** (Figure 1) or pure **2**.[27] Extensive searching located infrequent regions where the spacing of anthracene columns indicated mixed monolayer formation. A low resolution, constant height STM scan of one such region (Figure 3) revealed two types of 16-atom-long side-chain lamellae ($\sim$2.6 nm distance between anthracene columns): one formed by interdigitation of adjacent columns of **4** (red arrow in Figure 3; two adjoining side-chain columns with 2.2 nm anthracene spacing); the other formed by interdigitation of a column of **2** and a column of **4** (white arrow in Figure 3; 2.2 nm anthracene spacing in one adjoining side-chain column and 3.3 nm anthracene spacing in the other adjoining column). The regions that initially displayed mixed composition disappeared after samples sat at room temperature for many hours. Similar regions of mixed monolayers were never detected in samples annealed at elevated temperatures (45 °C) for 2 h.

Apparently, ($\omega \leftrightarrow 2$)-packing of [16^2] chains (**4**) with [$16^{3,14}$] chains (**2**) is significantly less favorable than ($\omega \leftrightarrow 2$)-packing of [$16^{2,15}$] chains (**1**) with [$16^{3,14}$] chains (**2**). In addition to the loss of attractive dipolar interactions, there are other structural factors that may contribute to segregation of the [16^2] and [$16^{3,14}$] chains of **4** and **2**. The monoether and diether side chains may experience loss of registration due to the different lengths and different numbers of C−C and C−O bonds. Alternatively, the side-chain shapes may differ due to curvature induced by ether oxygens.[28] The close proximity of ether groups in neighboring side chains of **1** and **2** may minimize packing

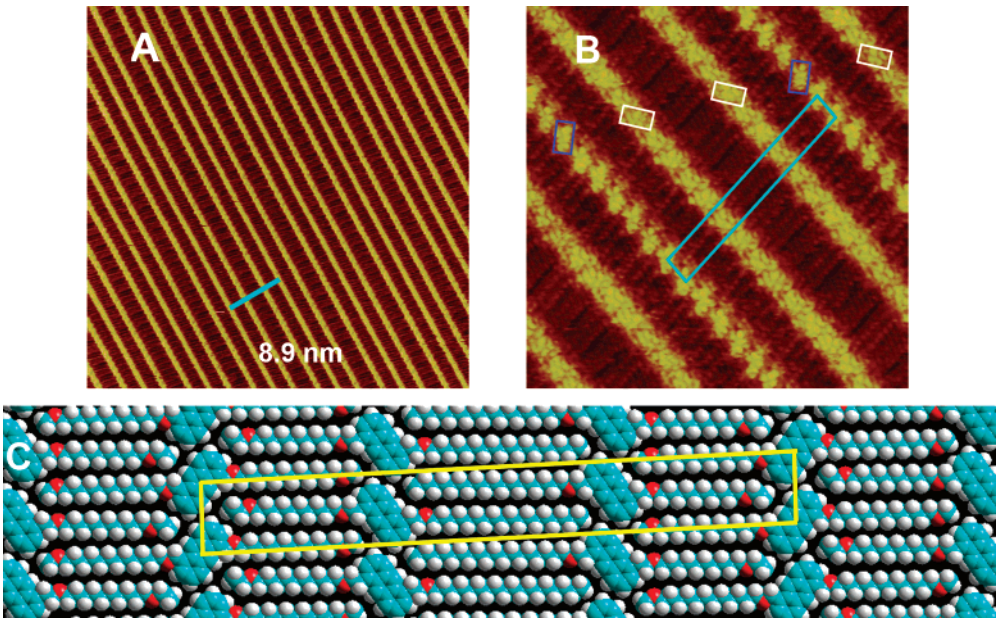

Figure 4. Constant current STM scans (0.1 nA, 1 V) of the monolayer formed by a phenyloctane solution of **3** and **2** (1:1) on HOPG. (A) The pattern of side-chain column widths from a 60 nm × 60 nm scan confirms self-assembly of a patterned, cocrystal monolayer, with a unit cell containing two molecules of **2** and one molecule of **3**. The light blue bar covers (approximately) one unit cell of the cocrystal. (B) A high-resolution 15 nm × 15 nm scan showing details of the molecules' adsorption orientations. The white (dark blue) boxes outline anthracenes from molecules of **2** (**3**). The light blue box outlines one unit cell of the cocrystal, with the triad repeat **3**-pR, **2**-pS-r, **2**-pS-l, where -r or -l indicates the longer [21^3] chain of **2** extending to the right or left of the anthracene column. (C) CPK cartoon of the monolayer assembled by **3** and **2**. The yellow box outlines the contents of one unit cell.

mismatch arising from bond length differences and side-chain curvature, in addition to providing two sets of favorable dipolar interactions per side chain. The failure to realize monolayer patterning from **4**/**2** mixtures underscores the critical need for side-chain recognition elements, in addition to chain length matching, to achieve designed cocrystal assembly.

Structure Control of Unit Cell Patterning. The patterned monolayer cocrystal assembled from molecules **1** and **2** on HOPG has three different side-chain column widths and a unit cell containing four molecules (tetrad repeat, Figure 2). The symmetrical anthracene derivative, **3**, has two copies of the [$16^{2,15}$] side chain complementary to the [$16^{3,14}$] side chain of **2**. Spontaneous patterning of **3**/**2** mixtures should form cocrystal monolayers with two distinct side-chain column widths, a unit cell containing three molecules and a triad repeat sequence. This prediction is confirmed by constant current STM scans of the monolayer formed on HOPG after application of phenyloctane mixtures of **3** and **2** (Figure 4).

The 60 nm scan in Figure 4A displays nine repetitions of the triad repeat sequence. Each triad has a column of **3** flanked on either edge by a column of **2**. The [$16^{2,15}$] chains from the central column of **3** are ($\omega \leftrightarrow 2$)-packed with the [$16^{3,14}$] chains from the adjacent columns of **2**, forming two, 2.7 nm wide side-chain columns lamella. As expected for ($\omega \leftrightarrow 2$)-packed even-length chains,[24a] molecules in the column of **3** adsorb to HOPG using the opposite enantiotopic face than used by molecules of **2** in the neighboring columns (Figure 4B). ($\omega \leftrightarrow 2$)-packing of [21^3] chains from adjacent columns of **2** form the 3.3 nm side-chain columns. These molecules of **2** adsorb to HOPG via the same enantiotopic face (Figure 4B), as expected for ($\omega \leftrightarrow 2$)-packing of odd-length chains. Despite using the same recognition elements as the **1**/**2** pair, the **3**/**2** pair forms a distinctly patterned monolayer cocrystal.

Conclusions

Molecular physisorption on graphite is predominantly driven by molecule−surface interactions.[29] Self-assembly of regular, 2-D monolayers on surfaces, particularly on atomically flat surfaces such as HOPG, is promoted by weak interactions among molecules. Even though the molecule−surface interactions are larger, the weaker, molecule−molecule interactions strongly influence monolayer assembly and morphology.[30] This work demonstrates that weak interactions, designed to introduce recognition and selectivity, can be combined with molecular shape (chain length) to direct self-assembly of patterned cocrystal monolayers. The systems employed here utilize dipole−dipole repulsions and attractions between ether functional groups to, respectively, destabilize single-component, ($\omega \leftrightarrow 2$)-packed side-chain columns and stabilize two-component, ($\omega \leftrightarrow 2$)-packed side-chain columns with alternating composition of adjacent side chains. This affords column-by-column control of the composition and morphology of the monolayer.

The patterned monolayers self-assembled from **3**/**2** mixtures and by **1**/**2** mixtures are distinct. Both molecule pairs employ chain length matching and dipolar interactions to drive pattern creation. The formation of two distinct, molecular structure-specific morphologies demonstrates that recognition and selection based on the (12-methoxydodecyloxymethyl)/(2-(10-ethoxydecyloxy)ethyl) ([$16^{2,15}$]/[$16^{3,14}$]) side-chain pair, in particular, and dipolar complementarity, in general, can be used to design patterned monolayer cocrystals with feature sizes as small as one molecule and unit cells that extend over many molecules. The two-component patterning demonstrated here can be extended to generate more complex monolayers. Ongoing efforts include (i) development of additional, complementary pairs of self-repulsive side chains to produce patterned monolayers assembled from three or more different molecules, (ii) replacing anthracene with "3D cores" to produce laterally and topographically patterned (3D) monolayers, (iii) development of side chains that promote "tiling", i.e., variation of molecular composition within a single column in addition to compositions of neighboring column.

Acknowledgment. The authors thank the National Science Foundation (CHE0616474) for financial support of this work and Dr. Vlastimil Fidler for advice and assistance.

Supporting Information Available: Synthesis and spectral data for compounds **1**−**4**. STM scans of the monolayer formed by (i) pure **2** on HOPG (low resolution); (ii) pure **2** on HOPG (high resolution with CPK packing model); (iii) **1** and **2** cocrystal (200 nm x 200 nm); (iv) pure **4** and the underlying HOPG surface in the same scan. This material is available free of charge via the Internet at http://pubs.acs.org.

JA075170R

(27) See the Supporting Information for STM scans of monolayers of pure **2**.
(28) Each CH_2−O bond, 1.43 Å, is shorter than a CH_2−CH_2 bond 1.54 Å. The angle between the mean chain directions of alkyl chains connected to a CH_2 group is 180°. The angle centered at an ether oxygen is 173°.
(29) Muller, T.; Flynn, G. W.; Mathauser, A. T.; Teplyakov, A. V. *Langmuir* **2003**, *19*, 2812−2821.
(30) Wintgens, D.; Yablon, D. G.; Flynn, G. W. *J. Phys. Chem. B* **2003**, *107*, 173−179.